Joint demosaicing and denoising of noisy bayer images with ADMM

Conference Paper · September 2017

DOI: 10.1109/ICIP.2017.8296823

5 authors, including:

Hanlin Tan
National University of Defense Technology
19 PUBLICATIONS **29** CITATIONS
SEE PROFILE

Xiangrong Zeng
National University of Defense Technology
26 PUBLICATIONS **71** CITATIONS
SEE PROFILE

JOINT DEMOSAICING AND DENOISING OF NOISY BAYER IMAGES WITH ADMM

Hanlin Tan, Xiangrong Zeng, Shiming Lai, Yu Liu and Maojun Zhang

College of Information System and Management, National University of Defense Technology, China

ABSTRACT

Image demosaicing and denoising are import steps of image signal processing. Sequential executions of demosaicing and denoising have essential drawbacks that they degrade the results of each other. Joint demosaicing and denoising overcomes the difficulties by solving the two problems in one model. This paper introduces a unified object function with hidden priors and a variant of ADMM to recover a full-resolution color image with a noisy Bayer input. Experimental results demonstrate that our method performs better than state-of-the-art methods in both PSNR comparison and human vision. In addition, our method is much more robust to variations of noise level.

Index Terms— Demosaicing, Denoising, Bayer image, ADMM

1. INTRODUCTION

Modern digital cameras have only one sensor to sample the intensity of three colors of light with a Bayer color filter array (CFA). In order to get a full-resolution color image, an interpolation process widely known as demosaicing is performed [1]. When the environmental light is not strong enough or the sensor area of camera (for instance, mobile phone cameras) is not large enough, the presence of noise in Bayer raw data is inevitable. However, a large fraction of demosaicing methods are developed under the unrealistic assumption of noise-free data [2]. The performances of those algorithms may degrade dramatically when the Bayer raw image is corrupted by noise. Therefore, a denoising step is also required.

Sequential demosaicing and denoising have essential drawbacks. Firstly, demosaicing itself is suffering from noise, and meanwhile, it alters the noise pattern and increases the difficulty for denoising. Thus joint demosaicing and denoising algorithms emerge accordingly. Condat et. al. introduced TV minimization to joint demosaicing and denoising [2]. Heide et. al. proposed a framework named FlexISP [3] to model and solve multiple categories of image restoration tasks including joint image demosaicing and denoising. Klatzer et. al. introduced a sequential energy minimization method [4] to solve the minimization problem of joint demosaicing and denoising. Gharbi et. al. developed a deep learning model [5] for joint demosaicing and denoising, which belongs to data driven methods. Chatterjee and Milanfar concluded in their work [6] that denoising was not dead since the performance of state-of-the-art methods, including BM3D, was still far from reaching the theoretical limit for a wide class of general images.

Based on those previous works, we improve joint demosaicing and denoising through combing multiple effective priors and introducing hidden priors in minimization model which is solved by the alternating direction method of multipliers (ADMM) . Experiments show that the proposed method provides better performance and robustness than state-of-the-art methods do given noisy Bayer raw images.

2. METHOD

2.1. Problem Formulation

Let Bayer image be denoted by $b \in R^n$ and the corresponding RGB image denoted by $x = [r^T, g^T, b^T]^T \in R^{3n}$. The image formation model is written as

$$b = Ax + \eta \tag{1}$$

where $A \in R^{n \times 3n}$ is the mosaic matrix which down samples RGB image x to Bayer image b, and $\eta \in R^n$ is the noise vector.

In the perspective of image recovery, joint demosaicing and denoising can be viewed as the inverse problem of (1). That is, the image recovery model can be expressed as

$$\min_x \|Ax - b\|_2^2 + T(x) \tag{2}$$

where function $T(x)$ represents the prior functions. Compared to conventional image recovery problems, (2) is much more ill-posed since we need to recover $3n$ variables from n known observations corrupted with noise. Therefore, how to choose a proper prior function $T(x)$ is the key to successful image recovery.

2.2. Priors

Image priors are based on image statistics and image structure. Before specifying the prior term, we discuss several as-

This work was partially supported by NSFC (Grant No. 61602494) and NUDT (Grant ZK160-03-16).

pects that denoising and demosaicing algorithms often take into consideration. Firstly, natural images have large parts of flat areas, where the smoothness assumption holds. However, natural images also have edges and details, where the smoothness assumption is violated. To ensure those details to be preserved, an edge-preserving denoising prior is required. Non-local denoising algorithms, including BM3D, do well in noise removal while keeping image details. The drawback is that non-local algorithms will produce artifacts in flat areas since the accumulated image patches are not exactly identical. Therefore, a smoothness prior and an edge-preserving denoising prior are complementary. Secondly, demosaicing is more than inferring $3n$ variables given n variables. The Bayer mosaic pattern provides us special structural information. Given n variables in matrix, manual designed interpolation filters contribute experiences of experts and stable performance. In contrast, iterative demosaicing methods are not recommended as priors in our framework since those methods adopt similar ideas of image recovery and cannot act as priors.

In order to maximize the recovery performance, we try to combine as many as possible priors known to be effective. The priors include but not limited to total variation (TV) [7] for smoothing, CBM3D [8] for denoising, cross-channel prior [9] for cross-channel inferring and conventional interpolation based demosaicing prior [10] taking advantage of structural information of Bayer pattern.

The image recovery model is specialized as

$$\min_x \|Ax-b\|_2^2 + \lambda_{tv}\|\nabla x\|_1 + \lambda_{bm3d} bm3d(x) + \lambda_{cc}\|Cx\|_1 + \lambda_{dm} demosaic(x) \tag{3}$$

In this model, the TV prior is specialized as

$$\|\nabla x\|_1 = \|H_1 x\| + \|H_2 x\|_1 \tag{4}$$

where $H_1, H_2 \in R^{3n\times 3n}$ are first-order derivatives enforcing horizontal and vertical smoothness.

The denoising prior $bm3d(x)$ is a hidden function without a closed form. It represents the prior contained in colored BM3D algorithm [8]. Fortunately, we are able to solve the minimization problem with the hidden prior function in subsection 2.3.

The cross-channel prior term is based on the assumption that pixel variations of three color channels at the same pixel location are likely to be the same. With arbitrary two channels l, k, the cross-channel prior can be expressed as

$$\begin{aligned} &\nabla i_k ./ i_k \approx \nabla i_l ./ i_l \\ \Leftrightarrow &\nabla i_k \cdot i_l \approx \nabla i_l \cdot i_k \end{aligned} \tag{5}$$

where$\cdot$ and $./$ are both element-wise operators. (5) derives the following matrix form [9]

$$\| \begin{bmatrix} R & & \\ & G & \\ & & B \end{bmatrix} x\|_1 \tag{6}$$

where

$$R = \begin{bmatrix} \beta_{rg}(D_g H_1 - D_{H_1 g}) \\ \beta_{rg}(D_g H_2 - D_{H_2 g}) \\ \beta_{br}(D_b H_1 - D_{H_1 b}) \\ \beta_{br}(D_b H_2 - D_{H_2 b}) \end{bmatrix} \tag{7}$$

$$G = \begin{bmatrix} \beta_{gb}(D_b H_1 - D_{H_1 b}) \\ \beta_{gb}(D_b H_2 - D_{H_2 b}) \\ \beta_{rg}(D_r H_1 - D_{H_1 r}) \\ \beta_{rg}(D_r H_2 - D_{H_2 r}) \end{bmatrix} \tag{8}$$

$$B = \begin{bmatrix} \beta_{gb}(D_g H_1 - D_{H_1 g}) \\ \beta_{gb}(D_g H_2 - D_{H_2 g}) \\ \beta_{br}(D_r H_1 - D_{H_1 r}) \\ \beta_{br}(D_r H_2 - D_{H_2 r}) \end{bmatrix} \tag{9}$$

In the definitions of matrices R, G, B, coefficients $\beta_{rg}, \beta_{br}, \beta_{gb}$ are cross-channel weights, D_v denotes the diagonal matrix of vector v, and H_1, H_2 are still first order derivative matrices.

The last but not least, the demosaicing prior is also a hidden function. This prior, whose implementation contains carefully designed interpolation filters [10], takes advantage of the structural information of Bayer pattern to infer the unknown pixels.

The proposed model (3) takes data loyalty, smoothness assumption, noise removal, color consistency and Bayer pattern into consideration. Good recovery results are possible if we properly select the prior weights.

2.3. Optimization with ADMM

Image recovery model (3) is a minimization model with one data term and multiple prior terms. The data term, TV term and cross-channel term are convex. However, whether the BM3D term and demosaicing term are convex or not is not determined.

Recent research works often use Alternating Direction Method of Multipliers (ADMM) [11] or primal-dual algorithm [12] to solve the type of minimization problem. We choose a variant of ADMM for simplicity in programming.

Suppose we have a minimization problem with J terms

$$\min_{z\in R^d} \sum_{j=1}^{J} g_j(H^{(j)} z) \tag{10}$$

where $g_j : R^{p_j} \to R$ are functions with closed form, $H^{(j)} \in R^{p_j \times d}$ are matrices and $p = p_1 + \cdots + p_J$. The general steps solving problem (10) are

1. Initialize u_0, d_0, μ with zero vectors.
2. Start iteration

$\zeta_k^{(j)} \leftarrow u_k^{(j)} + d_k^{(j)}, \quad j = 1, \cdots, J$
$\gamma_k \leftarrow \sum_{j=1}^{J} (H^{(j)})^T \zeta_k^{(j)}$
$z_{k+1} \leftarrow [\sum_{j=1}^{J} ((H^{(j)})^T H^{(j)})]^{-1} \gamma_k$
for $j = 1$ to J **do**
    $\nu_k^{(j)} \leftarrow H^{(j)} z_{k+1} - d_k^{(j)}$

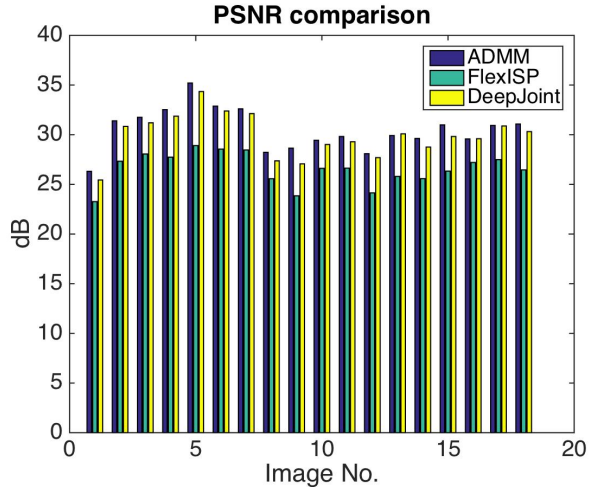

Fig. 1. PSNR Comparison. McMaster dataset with 18 images are tested. The original dataset images are groundtruths. The input noisy Bayer images are down-sampled from groundtruth images and corrupted with Gaussian white noise with standard deviation $\sigma = 15$. ADMM stands for the proposed method. FlexISP stands for Heide's method [3]. DeepJoint stands for Gharbi's method [5]. Our method is significantly better than comparative methods in most test cases.

6: $u_{k+1}^{(j)} \leftarrow \text{argmin}_v \frac{\mu}{2}\|v - \nu_k^{(j)}\|_2^2 + g_j(v)$

7: **end for**

8: $d_{k+1}^{(j)} \leftarrow d_k^{(j)} - (H^{(j)} z_{k+1} - u_{k+1}^{(j)}), \quad j = 1, \cdots, J$

3. Check stop criteria. If $|z_{k+1} - z_k| < \epsilon$, stop and turn to Step 4; Otherwise, let $k \leftarrow k + 1$, turn to Step 2.

4. Output z_{k+1} as a solution.

The detailed derivation can be found in [13]. Note in the *for* loop of Step 2, formula

$$u_{k+1}^{(j)} \leftarrow \text{argmin}_v \frac{\mu}{2}\|v - \nu_k^{(j)}\|_2^2 + g_j(v) \qquad (11)$$

corresponds to a restoration problem with v as the data term and $g_j(v)$ as the prior term, which suggests ADMM split a complicated minimization problem with multiple prior terms into multiple simple minimization problems with only one prior term. Therefore, the minimization problem with hidden BM3D prior can be solved by offering the denoising result of colored BM3D algorithm. The same applies to the demosaicing prior.

3. EXPERIMENT

We compare the proposed method with state-of-the-art methods on Kodak dataset and McMaster dataset [14], which contain 24 and 18 natural images, respectively. The Bayer images are down-sampled from groundtruth images. By adding Gaussian white noise to the Bayer images, we obtain the noisy Bayer inputs.

Table 1. Average PSNR Comparison on Two Datasets (dB)

Dataset	Noise Level	FlexISP [3]	DeepJoint [5]	ADMM (Ours)
Kodak (24 images)	$\sigma = 0$	**34.98**	33.88	31.63
	$\sigma = 5$	31.31	**33.07**	31.60
	$\sigma = 15$	26.67	**30.40**	30.16
	$\sigma = 25$	23.90	25.88	**28.38**
McMaster (18 images)	$\sigma = 0$	**35.18**	32.49	32.66
	$\sigma = 5$	31.17	32.01	**32.63**
	$\sigma = 15$	26.55	29.89	**30.50**
	$\sigma = 25$	23.73	26.13	**28.20**

The proposed ADMM algorithm outperforms compared algorithms on test cases with significant noise. However, It is not as good as FlexISP in test cases that are almost free from noise. In conclusion, our ADMM algorithm has good performance and is more robust to noise than compared algorithms.

Three algorithms, including FlexISP [3], deep joint method [5] and the proposed method, are compared using their source code on the same dataset. For all algorithms to be compared, the noise level of Gaussian noise is known. Our algorithm uses manually selected parameters and iterate 50 times for each input. In addition, the parameters of algorithms remain unchanged during the comparison.

Figure 1 illustrates the PSNR results on McMaster dataset with noise level $\sigma = 15$. It can be concluded that our method is significantly better than comparative methods in most test cases.

We also change the noise level of Bayer input images from $\sigma = 15$ to $\sigma = 5$ and $\sigma = 25$. Results for noise level $\sigma = 0$, which means the problem degenerates to a demosaicing problem, are also listed for reference. The average PSNR results are available in Table 1. When $\sigma = 25$, we achieve average 2.5 dB gains compared to DeepJoint and average 4.5 dB gains compared to FlexISP on Kodak dataset. As for McMaster dataset, we achieve 0.6 dB to 4.5 dB gains on noisy Bayer input. From the table we can conclude that the bigger the noise level is, the greater our algorithm outperforms compared algorithms. In other words, our method is much more robust to variations of noise level.

Figure 2 demonstrates the results visually. For Kodak dataset, the results of FlexISP and DeepJoint both suffer from artifacts such as visible noisy pixels or strange textures caused by denoising. The results of our ADMM method performs much better since they show less artifacts. FlexISP results degrade rapidly with visible noisy pixels as noise level increases. However, the results of ADMM remain good and stable, demonstrating the robustness of the proposed algorithm.

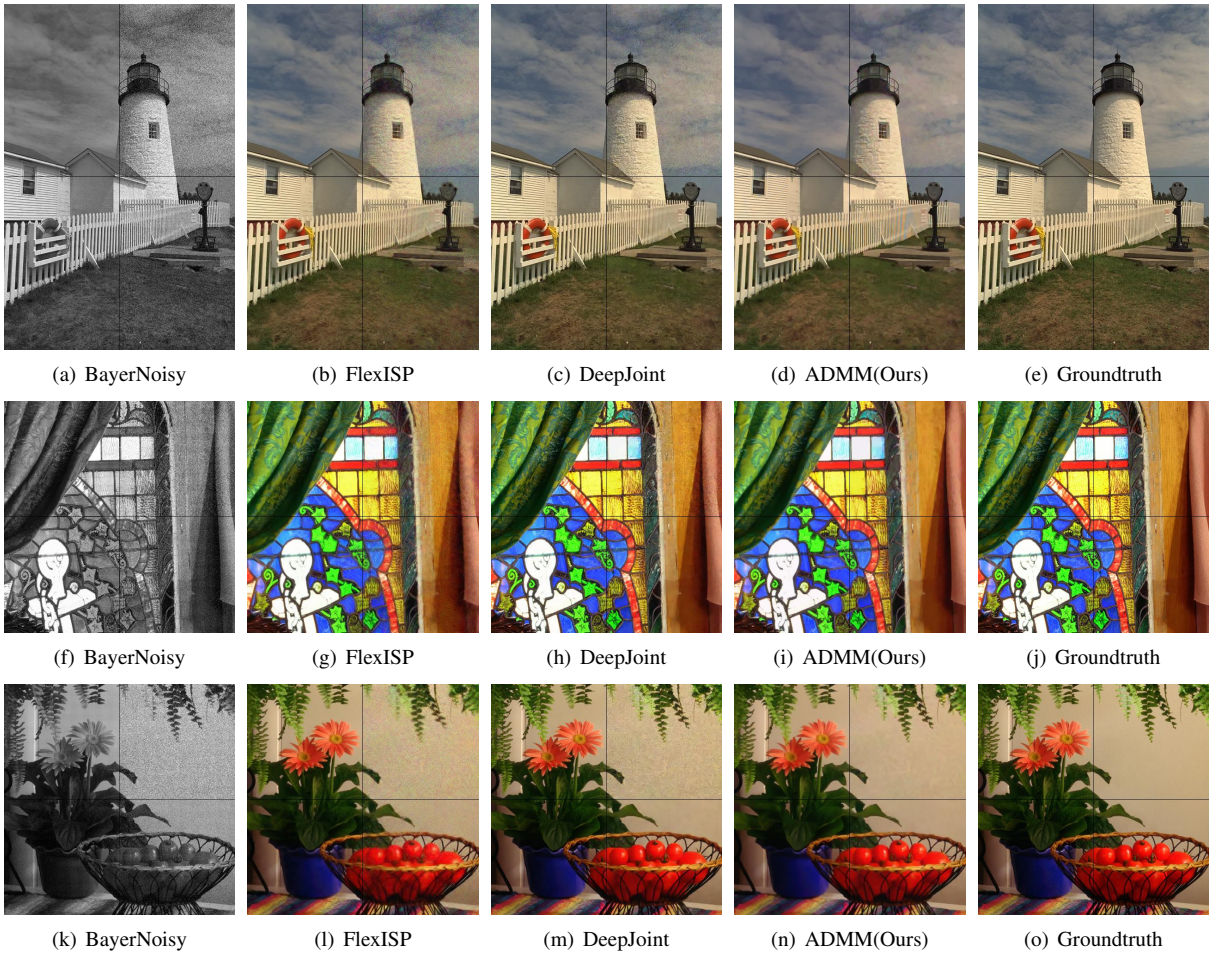

(a) BayerNoisy (b) FlexISP (c) DeepJoint (d) ADMM(Ours) (e) Groundtruth

(f) BayerNoisy (g) FlexISP (h) DeepJoint (i) ADMM(Ours) (j) Groundtruth

(k) BayerNoisy (l) FlexISP (m) DeepJoint (n) ADMM(Ours) (o) Groundtruth

Fig. 2. Visual Results. The first row and the last two rows of images are from Kodak and McMaster datasets, respectively. Each image is divided into four rectangular parts: Top-left, bottom-left, bottom-right and top-right correspond to noise levels $\sigma = 0, 5, 15, 25$, respectively. For Kodak dataset, the results of FlexISP and DeepJoint both suffer from artifacts such as visible noisy pixels or strange textures caused by denoising. The results of our ADMM method performs much better. FlexISP results degrade rapidly as noise level increases. However, the results of our ADMM algorithm remain good and stable. Note that during the whole experiment, parameters of all algorithms remain unchanged. You may need to enlarge the figure or see our supplementary material for more visual details.

4. DISCUSSION

We have presented an image recovery model for joint demosaicing and denoising. By introducing hidden priors, we are able to combine expert experience of demosaicing and denoising with natural image statistics, which dramatically increases the performance and robustness of joint demosaicing and denoising.

For future work, there are at least two directions: First, knowledge learned from statistical learning can be included in the model. On the one hand, statistical learning methods are able to find patterns that are difficult for humans to see. In Figure 2 (c), the color of the fence is pure, which is difficult to achieve for rule based model and demonstrates the advantage of statistical learning. On the other hand, some effective manually designed prior rules are difficult to be learned and kept by statistical learning. In Figure 2 (h) and (m), we observe strange color error of statistical learning methods, which demonstrates the disadvantage that those methods may violate simple and basic rules about Bayer pattern since the data-driven methods has no rules to follow. Therefore, we believe the combination of those two type of priors will lead to better performance. Second, the solver of the model requires optimizing. In our experiment, 50 iterations of our approach run about 900 seconds while deep learning model runs only about 4 seconds for an image of 0.4 mega pixels.

One limitation of our approach is that the theoretical convergence of ADMM is not determined since we do not know whether the hidden prior function is convex or not. However, our design of priors always converges in practice.

5. REFERENCES

[1] Xin Li, Bahadir Gunturk, and Lei Zhang, "Image demosaicing: A systematic survey," in *Electronic Imaging 2008*. International Society for Optics and Photonics, 2008, pp. 68221J–68221J.

[2] Laurent Condat and Saleh Mosaddegh, "Joint demosaicking and denoising by total variation minimization," in *2012 19th IEEE International Conference on Image Processing*. IEEE, 2012, pp. 2781–2784.

[3] Felix Heide, Markus Steinberger, Yun-Ta Tsai, Mushfiqur Rouf, Dawid Pajak, Dikpal Reddy, Orazio Gallo, Jing Liu, Wolfgang Heidrich, Karen Egiazarian, et al., "Flexisp: a flexible camera image processing framework," *ACM Transactions on Graphics (TOG)*, vol. 33, no. 6, pp. 231, 2014.

[4] Teresa Klatzer, Kerstin Hammernik, Patrick Knobelreiter, and Thomas Pock, "Learning joint demosaicing and denoising based on sequential energy minimization," in *Computational Photography (ICCP), 2016 IEEE International Conference on*. IEEE, 2016, pp. 1–11.

[5] Michaël Gharbi, Gaurav Chaurasia, Sylvain Paris, and Frédo Durand, "Deep joint demosaicking and denoising," *ACM Transactions on Graphics (TOG)*, vol. 35, no. 6, pp. 191, 2016.

[6] Priyam Chatterjee and Peyman Milanfar, "Is denoising dead?," *IEEE Transactions on Image Processing*, vol. 19, no. 4, pp. 895–911, 2010.

[7] Leonid I Rudin, Stanley Osher, and Emad Fatemi, "Nonlinear total variation based noise removal algorithms," *Physica D: Nonlinear Phenomena*, vol. 60, no. 1, pp. 259–268, 1992.

[8] Kostadin Dabov, Alessandro Foi, Vladimir Katkovnik, and Karen Egiazarian, "Color image denoising via sparse 3d collaborative filtering with grouping constraint in luminance-chrominance space," in *2007 IEEE International Conference on Image Processing*. IEEE, 2007, vol. 1, pp. I–313.

[9] Felix Heide, Mushfiqur Rouf, Matthias B Hullin, Bjorn Labitzke, Wolfgang Heidrich, and Andreas Kolb, "High-quality computational imaging through simple lenses," *ACM Transactions on Graphics (TOG)*, vol. 32, no. 5, pp. 149, 2013.

[10] Henrique S Malvar, Li-wei He, and Ross Cutler, "High-quality linear interpolation for demosaicing of bayer-patterned color images," in *Acoustics, Speech, and Signal Processing, 2004. Proceedings.(ICASSP'04). IEEE International Conference on*. IEEE, 2004, vol. 3, pp. iii–485.

[11] Stephen Boyd, Neal Parikh, Eric Chu, Borja Peleato, and Jonathan Eckstein, "Distributed optimization and statistical learning via the alternating direction method of multipliers," *Foundations and Trends® in Machine Learning*, vol. 3, no. 1, pp. 1–122, 2011.

[12] Eric Chu, Brendan ODonoghue, Neal Parikh, and Stephen Boyd, "A primal-dual operator splitting method for conic optimization," Tech. Rep., Stanford Internal Report, 2013.

[13] Mário AT Figueiredo and José M Bioucas-Dias, "Restoration of poissonian images using alternating direction optimization," *IEEE Transactions on Image Processing*, vol. 19, no. 12, pp. 3133–3145, 2010.

[14] Lei Zhang, Xiaolin Wu, Antoni Buades, and Xin Li, "Color demosaicking by local directional interpolation and nonlocal adaptive thresholding," *Journal of Electronic imaging*, vol. 20, no. 2, pp. 023016–023016, 2011.